Journal of Advances in Mathematics and Computer Science

26(6): 1-16, 2018; Article no.JAMCS.40185
ISSN: 2456-9968
(Past name: British Journal of Mathematics & Computer Science, Past ISSN: 2231-0851)

Incorporating Folding, Unfolding, Denaturation in a Mathematical Model for Cancer Spreading

T. A. Atabong[1*] and M. O. Oyesanya[2]

[1]Department of Mathematics, College of Science and Technology, Florida A&M University, 1516 Martin Luther King Bld, Fl 32307, USA.
[2]Department of Mathematics, University of Nigeria, Nsukka, Nigeria.

Authors' contributions

This work was carried out in collaboration between both authors. Author TAA designed the study, performed the statistical analysis, wrote the protocol, and wrote the first draft of the manuscript. Author MOO managed the analyses and part of the literature search of the study. Both authors read and approved the final manuscript.

Article Information

DOI: 10.9734/JAMCS/2018/40185
Editor(s):
(1) Kai-Long Hsiao, Associate Professor, Taiwan Shoufu University, Taiwan.
Reviewers:
(1) Grienggrai Rajchakit, Maejo University, Thailand.
(2) Hugo Cruz-Suárez, Benemérita Universidad Autónoma de Puebla, Mexico.
Complete Peer review History: http://www.sciencedomain.org/review-history/23638

Original Research Article

Received: 1st January 2018
Accepted: 7th March 2018
Published: 14th March 2018

Abstract

World known biological protein materials like arteries, bones, and tendons are constantly in a state of continuous stress due to their respective activities within the body. This stress will result in an increase in tissue residual temperature and consequently denaturation. The effects of denaturation on tumor initiation and progression are considered. All the parameters are integrated into a 9 step computational procedure, later transformed into a series of partial differential equations in time and space. A program was written to retrieve the steady states using parameters mined from existing and related models. The non-significant stable trivial steady state was observed to be driven unstable with an increase in the diffusion coefficient of the denatured cells. As denaturation increases, the progression of a tumor is exponential given a maker that denaturation favors the tumor population doubling model observed in many mathematical and biomedical studies. The outcome of this research can as well fit into other classes of tumors and will go a long way to contribute to the eventual eradication of tumor by suggesting elimination of stress of all forms in the body.

Keywords: Numerical algorithm; soft tissue; biological protein material; folding; denaturation.

**Corresponding author: E-mail: tagendia@gmail.com;*

1 Introduction

It has not been exclusively written in any literature whether the folding, unfolding, denaturation and destruction of protein molecules has a link to the formation of a tumor and probably progression. However, bones, tendons, enamel, and arteries are basically protein materials [1]. Most of these materials play a significant role in the overall body maintenance and can cause life-threatening diseases like prostate cancer if some of their functions are derailed [2]. Prostate cancer is known to be the most common malignancy and the second leading cause of male cancer deaths in the United States [3]. Even though the precise mechanism involved in prostate carcinogenesis remains not certain, it is likely that there are certain genetic alterations in prostatic epithelial cells that permit them to proliferate and metastasize [4]. A work by Deng et al. [5], suggested that Bone morphogenetic proteins (BMPs) are potential regulators of prostate cancer cell growth and metastasis. In addition to prostate cancer, breast cancer, blood cancer and malignant primary bone tumors can all results primarily from the destruction of biological protein materials. Heat, as well as high temperatures, have been linked to causing foldings, denaturation and possibly the destructions of biological protein materials [6].

Models have been used to explain protein denaturation, folding, unfolding [7,8], soft tissue mechanics in cancerogenesis [9], and different illnesses cause as a result of soft tissue destruction [9-11]. Most of these models are subject to the fact that, the destruction of a soft tissue can be of significant damage to the cells, tissues, and organs [12,13]. The main mechanisms associated with these destruction remains a frontier [14]. In this light, we incorporate denaturation, unfolding, folding, destruction of soft tissues as a means to model the initiation, migration, and metastasis of tumors. Similar models to this models are found in [15-17]. These models considered the spread of cancer as result of recruiting normal cells into cancer cell using the Diffusive-predator-prey concept like those in [18]. Each of these models shows some degree of coupling between reacting components or species but however, are using different specific properties for the emerge of cancerous cells. The models failed to integrate the notion of soft tissue mechanics and biological protein materials. For example, the models in [15-17,19] have both the normal, cancerous cells and the acidic content all interacting. In the process, while the acidic content favor the development of more acidic cells, it reversely affects the normal cells by killing them. These models used the assumption of cellular respiration as the only reason for increase initiation of acidic content. They fail to show how these acidic content is generated from metabolic activities. The present model not only consider the aspect of respiration, but equally took in consideration the surrounding medium that can initiate metabolic processes. The current increasing incidence rate of cancer [20] can be overcome with the integration of these concepts. We introduce the model in section 2 below.

2 Computational Transformation and Block Flow Diagram

Cells are the building blocks for tissues and organs. From the three (3) reacting species reaction-diffusion system of Gatenby & Galinski [19], we developed a five (5) reacting species model involving, Normal cells, the Tumor cells, the Denatured (fracture) cells the Excess H+ concentration and the tissue reserved temperature. BMP are constantly in a state of stress in order to meet up with the day-to-day activities (functions) of the different organs making up life [21]. The main organs of concern in this model are the arteries, the bones, and the tendons shown in Fig. 1. below

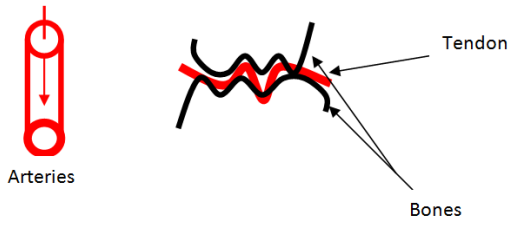

Fig. 1. InFlow of blood in

This model is built from the fact that the artery as a biological protein material is constantly carrying blood from the heart to the tissues and organs of the body. The flow of blood through the arteries obeys the continuity equation [22]. During periods of abnormal heartbeats, Saxon and colleagues [23] explained that the pressure of blood in the arteries are either higher or lower than normal. The arteries always expand and contract to normalize the pressure of the blood at any point in time by increasing or reducing the surface area or viscosity [22]. Like the arteries, the tendons helps to prevent friction between alternate bones by constantly pulling the bones apart during load (and stress). The bones help to keep the body upright and stable hence constantly changing its form so as to overcome the load demand of the body [21]. These tissues are all made of protein, hence the name soft tissue or biological protein materials. These tissues constantly remodel themselves in a way as to carry out their respective function. According to Saxons and colleagues, [23] a brief eliciting failure in the neighborhood of 3 to 300 seconds as an exponential decay of muscular performance. This decay in muscular performance can be seen as a precursor for the initiation and development of tumor in the same way cracks and deformation developed with elastic materials when the elastic limit is exceeded. These components are related to an energy flow chart as follows;

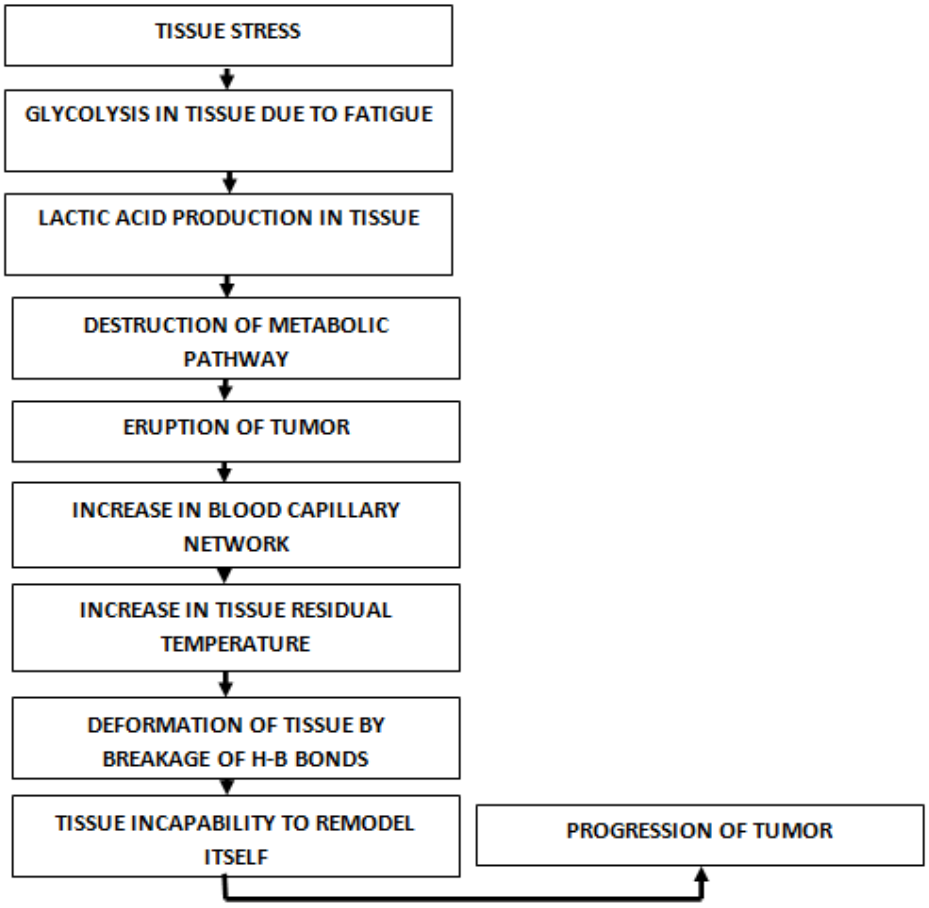

Chart 1. Flowchart of tumor attack and progression

3 Derivation of Parameters of Model

To formalize the model, consider N(t,x) to be the proportion of normal cells and M(t,x) the proportion of tumor cells all measure in cell/cm^3, H^+ (t,x), the concentration of liberated hydrogen ion from acid measured

in Molar (M) [20]. Let F(t,x) be the proportion of fractured (or deformed) cells and T(t,x) be the residual temperature in the tissue at time t. Define K_N, K_M, and K_P to be the carrying capacities [24] of the Normal cells, the tumor cells, and the fractured cells. Like the Normal cells, we measure the carrying capacity in cells/cm^3. Let K_1 and K_2 be the rates of forward and backward reactions for the denaturation and renaturation of protein in the cells measured in cm/s^2. Standard reaction predicts that [25,26],

$$K_1 = \gamma_1 e^{-E_1/RT}, K_2 = \gamma_2 e^{-E_2/RT}. \tag{1}$$

Where E_1 and E_2 are energy barrier to the forward and backward reactions respectively, R is the Rydberg's constant [27] and T is the temperature in Kelvin. The coefficients γ_1, γ_2 are called the stoichiometric constant. Let r_N and r_M be respectively the normal rate of the multiplicity of normal and tumor cells measure in 1/s. Let a_1 and a_2 be the constant parameter representing the resistance [28] to normal cellular fracture and tumor and tumor cell fracture respectively. Let b_1, b_2, b_3, b_4, and b_5 be the diffusion coefficients of the respective cells measured in cm^2/s [17]. Let a_c be the rate of production of lactic acid with Mcm^2/cell.s as the unit of measurement [20]. Suppose d is a function of the density and heat capacity of the tissue in KJ/Mol.K [29]. We defined $\Delta H_1, \Delta H_2$ to be the heat released during the denaturation and renaturation processes, a process typically measured in KJ/Mol.K. [25]. Let χ and V_0 be the bond breaking rate and the natural bond breaking speed respectively [30]. Let a_d be the acid regulation rate [31] or rate of re-absorption of acid by the tumor cells then the mathematical model can be represented as follows;

$$\frac{\partial F}{\partial t} = b_1 \nabla^2 + \chi \frac{K_1 NM}{V_0} - \frac{K_2}{g_0} F \tag{2}$$

$$\frac{\partial N}{\partial t} = b_2 \nabla^2 N - K_1 NM + r_N \left(1 - a_1 \frac{MF}{K_M K_F}\right) N - r_{1N} H^+ N \tag{3}$$

$$\frac{\partial M}{\partial t} = b_3 \nabla^2 M - K_2 F + r_M \left(1 - a_2 \frac{NF}{K_N K_F}\right) M \tag{4}$$

$$\frac{\partial H^+}{\partial t} = b_4 \nabla^2 H^+ + a_c M - a_d H^+ + r_{1N} H^+ N \tag{5}$$

$$d \frac{\partial T}{\partial t} = b_5 w_0 \nabla^2 T - \Delta H_1 K_1 NM - \Delta H_2 K_2 F + J_{TOT}.E \tag{6}$$

The off rate and the bond breaking speed defined by Markus and Ackbarow [32,30] is given respectively by,

$$\chi = w_0 .e[-(E_b - F_b .x_b \cos\theta)/k_b T]$$
$$V_0 = w_0 .x_b .e^{-E_b/k_b T} \tag{7}$$

and described how quick and often a bond is breaking per unit time. The force used in breaking the hydrogen bonds. The bond breaking speed because of the applied force has also been deduced bond breaking rate and is given by;

$$V_1 = w_0 .x_b .e[-(E_b - F_b .x_b \cos\theta)/k_b T]. \tag{8}$$

In this case, we represent F_b is the applied force, w_0 the vibration frequency, θ the angle between the bonds, x_b the horizontal displacement of the bond.

We defined the following quantities,

$$p = \frac{F}{F_0}, u = \frac{N}{N_0}, v = \frac{M}{M_0}, w = \frac{T}{T_0}, q = \frac{H}{H_0}, \tau = \frac{t}{t_0}, \xi = \frac{x}{L} \tag{9}$$

Substituting this into the above equations lead to the system,

$$\frac{\partial p}{\partial \tau} = \frac{t_0 b_1}{L^2}\frac{\partial^2 p}{\partial \xi^2} + \chi \frac{t_0 K_1 N_0 M_0}{F_0 V_0} uv - t_0 K_2 p \tag{10}$$

$$\frac{\partial u}{\partial \tau} = \frac{t_0 b_2}{L^2}\frac{\partial^2 u}{\partial \xi^2} - t_0 K_1 M_0 uv + r_n t_0 u\left(1 - \frac{a_1 M_0 F_0}{K_m K_p} vp\right) - t_0 r_{1N} H_0 uq \tag{11}$$

$$\frac{\partial v}{\partial \tau} = \frac{t_0 b_3}{L^2}\frac{\partial^2 v}{\partial \xi^2} - \frac{t_0 K_2 F_0}{M_0} p + r_M t_0 v\left(1 - \frac{a_2 N_0 F_0}{K_N K_p} up\right) \tag{12}$$

$$\frac{\partial q}{\partial \tau} = \frac{t_0 b_4}{L^2}\frac{\partial^2 q}{\partial \xi^2} + \frac{t_0 a_c M_0}{H_0} v - a_d t_0 q + t_0 r_{1N} N_0 uq \tag{13}$$

$$\frac{\partial w}{\partial \tau} = \frac{t_0 b_5}{dL^2}\frac{\partial^2 w}{\partial \xi^2} - \frac{t_0 K_1 N_0 M_0 \Delta H_1}{dT_0} uv - \frac{t_0 K_2 F_0 \Delta H_2}{dT_0} p + \frac{J_{tot}.E.t_0}{Dt_0} \tag{14}$$

Considering that the cell is not reacting to any external electromagnetic force and therefore will not be producing current, we may set the last term of eq 14 to zero,

$$\frac{J_{tot}.E.t_0}{Dt_0} = 0. \tag{15}$$

Setting $t_0 = \frac{L^2}{b_1}$, we get,

$$\frac{\partial p}{\partial \tau} = \frac{\partial^2 p}{\partial \xi^2} + \chi \frac{t_0 K_1 N_0 M_0 L^2}{F_0 V_0 b_1} uv - \frac{t_0 K_2 L^2}{b_1} p \tag{16}$$

$$\frac{\partial u}{\partial \tau} = \frac{b_2}{b_1}\frac{\partial^2 u}{\partial \xi^2} - \frac{t_0 K_1 M_0 L^2}{b_1} uv + \frac{r_n t_0 L^2}{b_1} u\left(1 - \frac{a_1 M_0 F_0}{K_m K_p} vp\right) - \frac{t_0 r_{1N} H_0 L^2}{b_1} uq \tag{17}$$

$$\frac{\partial v}{\partial \tau} = \frac{b_3}{b_1}\frac{\partial^2 v}{\partial \xi^2} - \frac{t_0 K_2 F_0 L^2}{M_0 b_1} p + \frac{r_M t_0 L^2}{b_1} v\left(1 - \frac{a_2 N_0 F_0}{K_N K_p} up\right) \tag{18}$$

$$\frac{\partial q}{\partial \tau} = \frac{b_4}{b_1}\frac{\partial^2 q}{\partial \xi^2} + \frac{t_0 a_c M_0 L^2}{H_0 b_1} v - \frac{a_d t_0 L^2}{b_1} q + \frac{t_0 r_{1N} N_0 L^2}{b_1} uq \tag{19}$$

$$\frac{\partial w}{\partial \tau} = \frac{b_5}{d b_1}\frac{\partial^2 w}{\partial \xi^2} - \frac{t_0 K_1 N_0 M_0 \Delta H_1 L^2}{d T_0 b_1} uv - \frac{t_0 L^2 K_2 F_0 \Delta H_2}{d T_0 b_1} p \tag{20}$$

By defining new set of dimensionless parameters to scale the system of equations above we obtain the following parameters;

$$s_i = \frac{b_{i+1}}{b1}, i = 1-4 \quad , \quad \alpha = \chi \frac{L^2 K_1 N_0 M_0}{b_1 F_0 V_0} \quad , \quad H_0 = \frac{b_1}{L^2 r_{1N}}, \quad r = \frac{r_M}{r_N} \quad , \quad \beta = \frac{K_2}{r_N g_0} \quad ,$$

$$\alpha_1 = \frac{a_c M_0 L^4 r_{1N}}{b_1^2} \quad , \quad \theta_1 = \frac{M_0 F_0}{K_M K_p} \quad , \quad \theta_2 = \frac{N_0 F_0}{K_N K_p} \quad , \quad \theta_3 = \frac{L^2 r_{1N} N_0}{b_1} \quad , \quad \beta_3 = \frac{\Delta H_2 K_2 F_0}{\Delta H_1 K_1 N_0 M_0} \quad ,$$

$$T_0 = \frac{\Delta H_1 K_1 N_0 M_0 L^2}{d b_1} \quad , \beta_2 = \frac{a_c L^2}{b_1} \quad , \alpha_3 = \frac{L^2 K_1 M_0}{b_1} \quad , \alpha_4 = \frac{K_2 F_0 L^2}{M_0 b_1} \quad , y_1 = \frac{w_0}{d} \quad .$$

Substituting these parameters into the system eq 16-20, we obtain,

$$\frac{\partial p}{\partial \tau} = \frac{\partial^2 p}{\partial \xi^2} + \alpha uv - \beta p$$

$$\frac{\partial u}{\partial \tau} = s_1 \frac{\partial^2 u}{\partial \xi^2} - \alpha_3 uv + u\left(1 - a_1 \theta_1 vp\right) - uq$$

$$\frac{\partial v}{\partial \tau} = s_2 \frac{\partial^2 v}{\partial \xi^2} - \alpha_4 p + rv\left(1 - a_2 \theta_2 up\right) \tag{21}$$

$$\frac{\partial q}{\partial \tau} = s_3 \frac{\partial^2 q}{\partial \xi^2} + \alpha_1 v - \beta_2 q + \theta_3 uq$$

$$\frac{\partial w}{\partial \tau} = s_4 y_1 \frac{\partial^2 w}{\partial \xi^2} - uv - \beta_3 p$$

The system eq 21 is the non-dimensional system on which we shall analyze for tumor outbreak and progression. We can typically study this system with zero flux boundary condition signifying the fact the impossibility for the tumor to extend to other tissues of the body.

4 Analysis of Steady States

We consider all three possibilities of steady states. We looked at the spatial, the temporal and the spatiotemporal steady states conditions. It is clear that the solution of the equation of (21) exist continuity of functions and boundary conditions.

Setting the spatial derivatives in 21 to zero gives the system;

$$\begin{aligned}
\frac{\partial p}{\partial \tau} &= \alpha uv - \beta p \\
\frac{\partial u}{\partial \tau} &= \alpha_3 uv + u\left(1 - a_1\theta_1 vp\right) - uq \\
\frac{\partial v}{\partial \tau} &= -\alpha_4 p + rv\left(1 - a_2\theta_2 up\right) \\
\frac{\partial q}{\partial \tau} &= \alpha_1 v - \beta_2 q + \theta_3 uq \\
\frac{\partial w}{\partial \tau} &= -uv - \beta_3 p
\end{aligned} \tag{22}$$

which is satisfied by the solution is given by;

$$\begin{aligned}
p &= \frac{\alpha uv}{\beta} - p_0 e^{-\beta\tau} \\
u &= u_0 e^{\left[1-\left(a_3 v + a_1\theta_1 vp + q\right)\right]\tau} \\
v &= \frac{\alpha_4 p}{r\left(1 - a_2\theta_2 up\right)} + v_0 e^{r\left(1-a_2\theta_2 up\right)\tau} \\
q &= \frac{-\alpha_1 v}{\theta_3 u - \beta_2} + q_0 e^{\left(\theta_3 u - \beta_2\right)\tau} \\
w &= \left(-uv - \beta_3 p\right)\tau
\end{aligned} \tag{23}$$

From the steady-state coupled solution in (23), one can easily see that the trivial steady state satisfy this relationship. All possible values of this steady state depend not only on the parameters but also on the values of the other variables. Hence there exit parameter values where all five variables can coexist. The negative nature of w is an indication that at all temperatures, heat is always released in the tissues.

Secondly, the temporal dynamics has steady states satisfying the system of differential equations,

$$\frac{\partial^2 p}{\partial \xi^2} = -\alpha uv + \beta p$$

$$s_1 \frac{\partial^2 u}{\partial \xi^2} = \alpha_3 uv - u(1 - a_1\theta_1 vp) + uq$$

$$s_2 \frac{\partial^2 v}{\partial \xi^2} = \alpha_4 p - rv(1 - a_2\theta_2 up) \tag{24}$$

$$s_3 \frac{\partial^2 q}{\partial \xi^2} = -\alpha_1 v + \beta_2 q - \theta_3 uq$$

$$s_4 y_1 \frac{\partial^2 w}{\partial \xi^2} = uv + \beta_3 p$$

We seek solution of 24 to satisfy the zero-flux boundary condition, in the form,

$$(p, u, v, q, w) = (p_0 \cos n\pi x, u_0 \cos m\pi x, v_0 \cos i\pi x, q_0 \cos j\pi x, \cos n\pi x, w_0 \cosh \pi x,).$$

This solution guarantee the periodic nature of the interactions between the cancerous cells with the normal as well as fractured cells. The constants p_0, u_0,v_0,q_0,w_0 are real numbers, representing the initial scaled values of the cells for each interacting species while *m, n, I, j, h* are integers. Interactions between the integers *m, n, I, j, h* shows that for $h=n$ which is equivalent to a direct relationship between the rate of denaturation (or fracture) and the reserve temperature, we see that the parameter *n* or *h* can only take values given by,

$$n^2 = \frac{p_0(\beta - \beta_3\alpha)}{\pi^2(p_0 + s_4 y_1 w_0)} \tag{25}$$

Also, since the production of H^+ is tantamount to the tumor growth, setting $i=j$, we get the relationship,

$$m = Arc\cos\left[\frac{s_3 q_0 j^2\pi^2 + a_1 v_0 - \beta_2 q_0}{-\theta_3 q_0 u_0}\right]. \tag{26}$$

This steady state solution is periodic and we reckon that this solution will be stable to small amplitude.

Thirdly, spatially uniform steady state of 21 satisfy the equations,

$$\begin{aligned}
&\alpha uv = \beta p \\
&-\alpha_3 uv + u(1 - a_1\theta_1 vp) = uq \\
&\alpha_4 p = rv(1 - a_2\theta_2 up) \\
&\alpha_1 v + \theta_3 uq = \beta_2 q \\
&-uv = \beta_3 p
\end{aligned} \tag{27}$$

From where we obtain a relationship between the fracture cells and the normal cells given by,

$$p = \frac{1-q}{\frac{\alpha_3 \beta}{u\alpha} + a_1\theta_1 v} \quad . \tag{28}$$

Increasing the normal cells increases the tendency of denaturation keeping all other things constant. This shows that we are not on the wrong track as it can be linked to fat individuals developing a tumor of the bone and prostate easily. Equation (28) also shows that the increase in tumor cells reduces the proportion of fractured cells. This is in line with the fact that the tumors are more prepared and happy to consume fracture cells more than the normal cells. In another way, the deformation of normal cells increases the rate of spreading of the tumor cells.

Solving for the steady states shows that, there exist only two realistic steady states which are the trivial steady state $p = 0, u = 0, v = 0, q = 0, w =< w >$ and the steady state,

$$p = \frac{\alpha\mu}{\beta}, u = 1, v = \mu, q = \frac{\alpha_1 \mu}{\beta_2 - \theta_3}, w =< w > \quad . \tag{29}$$

Since w does not exclusively appear in the steady-state equations, it means that there is always a reserved temperature for cellular activities. Thus the steady state depends meanly on the deformed tissues, the normal cells, the tumor cells and the concentration of H^+.

The parameter μ in (29) is given by;

$$\beta \frac{-(\alpha_3 + \alpha_1) + \sqrt{(\alpha_3 + \alpha_1)^2 + \frac{4\alpha a_1\theta_1}{\beta}(\beta_2 - \theta_3)^2}}{2\alpha a_1\theta_1(\beta_2 - \theta_3)} \quad \text{if } \beta_2 > \theta_3$$

and (30)

$$\beta \frac{-(\alpha_3 + \alpha_1) - \sqrt{(\alpha_3 + \alpha_1)^2 + \frac{4\alpha a_1\theta_1}{\beta}(\beta_2 - \theta_3)^2}}{2\alpha a_1\theta_1(\beta_2 - \theta_3)} \quad \text{if } \beta_2 < \theta_3 .$$

5 Numerical Determination of Frequency of Folding, Unfolding, Denaturation, and Tumor

We wrote codes to simulate equation (25) for different integer values of n in order to determine when will the fracture cells result in tumors and calculate the tumor doubling growth rate. Three sets of essential parameter values were used for the simulations in order the compare the rates of cancer progression. The parameter set and the values as found on the equations were gotten from literatures on cancer. These parameters are presented in Table 1 below.

Table 1. Parameter for numerical simulation as obtained from literatures indicated

Set one		Set two		Set three	
Parameter	**Parameter value**	**Parameter**	**Parameter value**	**Parameter**	**Parameter value**
Mode n=0	pi=22/7 p0=0.005 s4 = 84.1667 y1 = 0.0490 w0=0.08	Mode n=0	pi=22/7 p0=0.5 s4 = 84.1667 y1 = 0.0490 w0=0.8	Mode n=0	pi=22/7 p0=0.005 s4 = 0.004 y1 = 0.090 w0=0.08
Mode n=2	pi=22/7 p0=0.005 s4 = 84.1667 y1 = 0.0490 w0=0.08	Mode n=2	pi=22/7 p0=0.5 s4 = 84.1667 y1 = 0.0490 w0=0.8	Mode n=2	pi=22/7 p0=0.005 s4 = 0.004 y1 = 0.090 w0=0.08
Mode n =10	pi=22/7 p0=0.005 s4 = 84.1667 y1 = 0.0490 w0=0.08	Mode n =10	pi=22/7 p0=0.5 s4 = 84.1667 y1 = 0.0490 w0=0.8	Mode n =10	pi=22/7 p0=0.005 s4 = 0.004 y1 = 0.090 w0=0.08
Mode n=25	pi=22/7 p0=0.005 s4 = 84.1667 y1 = 0.0490 w0=0.08	Mode n=25	pi=22/7 p0=0.5 s4 = 84.1667 y1 = 0.0490 w0=0.8	Mode n=25	pi=22/7 p0=0.005 s4 = 0.004 y1 = 0.090 w0=0.08
Mode n=100	pi=22/7 p0=0.005 s4 = 84.1667 y1 = 0.0490 w0=0.08	Mode n=100	pi=22/7 p0=0.5 s4 = 84.1667 y1 = 0.0490 w0=0.8	Mode n=100	pi=22/7 p0=0.005 s4 = 0.004 y1 = 0.090 w0=0.08

6 Results and Discussion

A simulation was carried out with the stated parameters and results presented as follows:

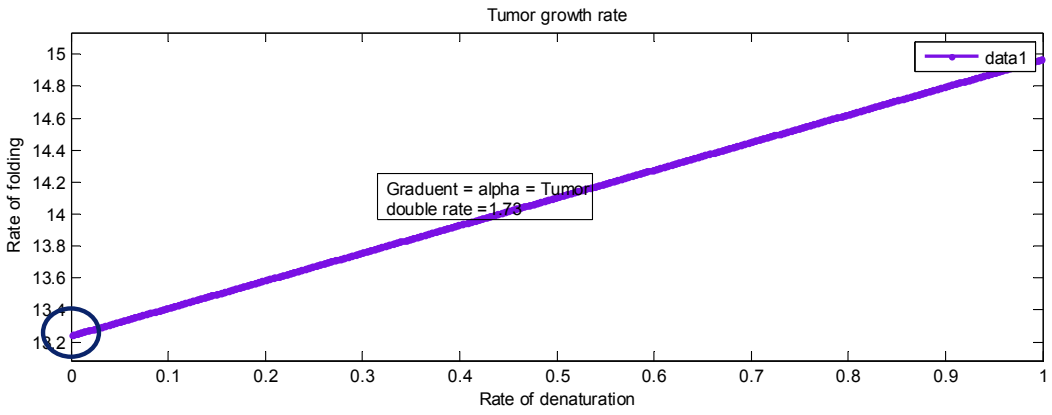

Fig. 2. A plot of Rate of folding against the rate of denaturation showing the tumor growth doubling rate of 1.73. and the tumor no growth unfolding rate of 13.23.

From Fig. 2, It can be inferred that during the transformation process, as normal protein cells get unfolded due to high reserve temperature, if the temperature is returned to normal, the backward reaction reset the cells into folding as a result of the production of more normal cells. If the folding rate is equivalent to 13.23, then no denatured cells will be transformed into tumor cells. The tumor will not progress. If the folding rate increases, then more energy is produced from the backward reaction as a result, the denaturated cells get fractured and transform into tumor cells. Therefore it is necessary to maintain the renaturation process gradually instead of abruptly. That is the temperature changes cause a denaturation, it is necessary to reverse the temperature gradually than to get into automatic reduction. Automatic reversal only lead to more problem. naturally, if the temperature increases and the body becomes very hot, it is not a good indication to get into a very cool environment in order to reduce the body temperature. The reversal process needs to be slow and persistent. This is in line with the number of deaths recorded as a result of automatic temperature deviation [33]. External climate change is a cause of serious health hazard and has resulted in a number of deaths in the united states. Extreme weather events are becoming more intense and frequent[34] Robine and colleague [35]; Hales et al. [36-38]. This result is a prove (confirmation) of the fact that extreme weather condition has the potentials of causing cancer of the skin, breast, and brain.

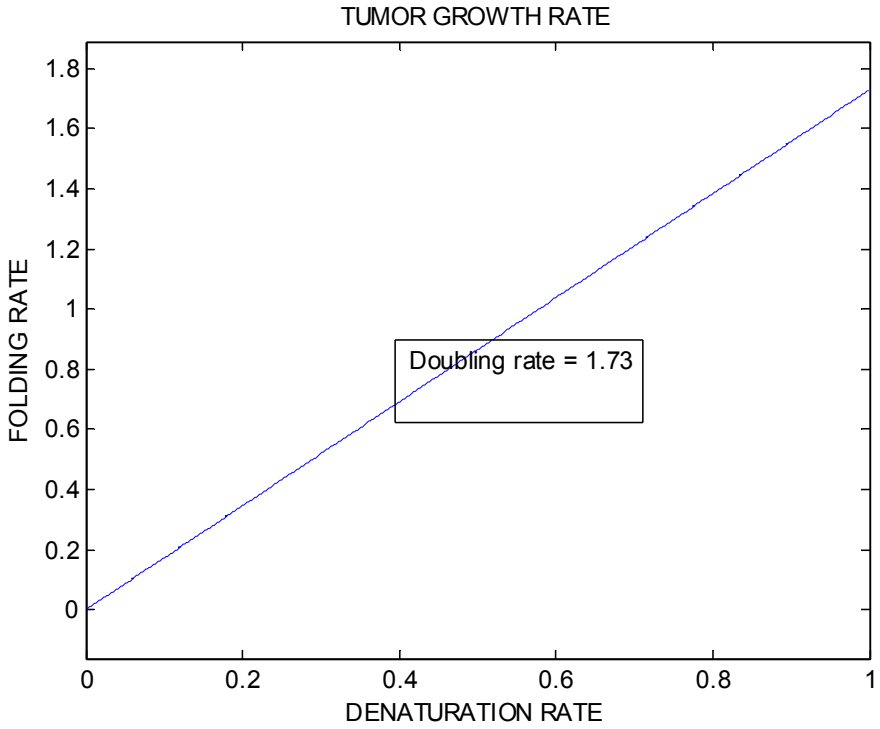

Fig. 3. Folding rate against denaturation rate for n=0

Different simulations were done for different values of *n* and found that as the mode number increase, the initial folding rate which is required to start the progression of tumor also increase without changing the doubling rate. Since the mode number *n* is a function of the periods the next rise in reserve temperature is felt, in 1 second. Therefore the more frequently the reserve temperature increases, the high the rate of folding and the more the denaturation increases [39,40] and consequently the progression of cancer. This is an extra boost to the volume of knowledge on cancer known, that lactic acid which is the source of cancer initiation and progression as found in [22] or a contributing factor in the initiation of cancer as found in [15]. The temperature-induced denaturation and consequently fracture of cells, promotes the progression of cancer and is therefore a reason of the abnormal multiplication of cells as found in all forms of cancer [41].

On the parameter set two, a similar plot to Fig. 2 was gotten with the exception of the doubling rate of the tumor which was found to be 1.93 as against 1.73 using parameter set one. This change is coming principally from the increase in the initial number of fractured cells. The plot is presented in Fig. 4 below.

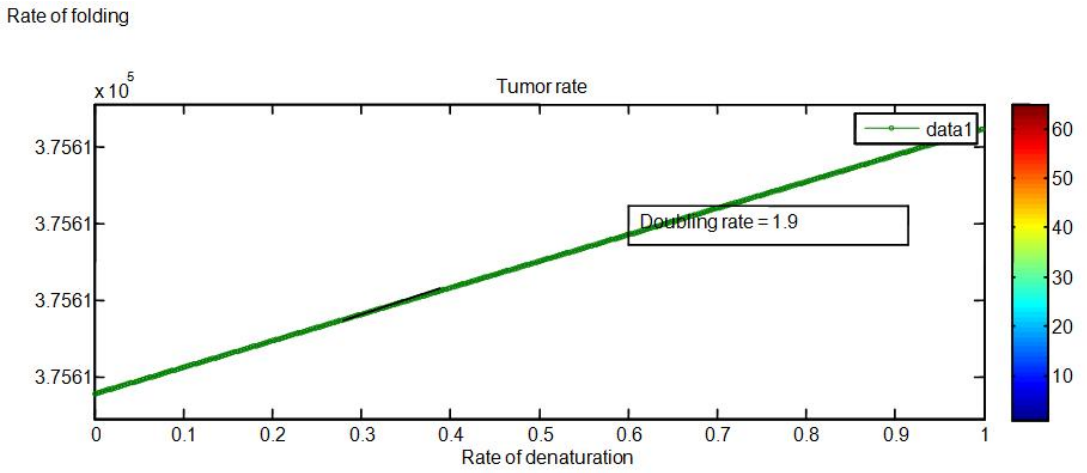

Fig. 4. Plot of Rate of denaturation as against rate of folding

The folding rate required to initialize tumor development also increase in this case with a superior value of $3.756x10^5$. Therefore parameter set two gives a slightly different progression of cancer rates and can be used as a benchmark for the fighting of the progression of the abnormal multiplicity of cells. Drugs and immunologist may use this values for determined the appropriate doses for the treatment of cancer.

When we change the parameter to set three, our simulation shows more interesting pattern as shown in Fig. 5 below,

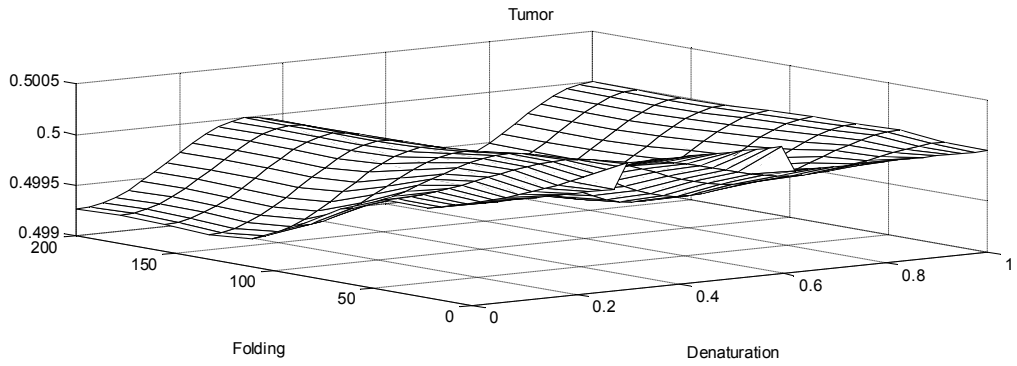

Fig. 5. A plot of denaturation against folding for tumor development

From Fig. 5, it is obvious that denaturation increase tumor development as low as for initial folding rate of 50 cells per centimeter cube. As the folding increases, tumor development drops from a pick value of 0.5 to a value of 0.49. At a denaturation rate of 0.4 and folding of 50 tumor growth rate increases shapely then drops zero. This can only occur when the body immune system fights back to destroy the tumor cells. This, however, does not last as the tumor immediately increase when the denaturation rate systematically increases 0.6 to 1. This goes to confirm statistics that in an event of a tumor outbreak, if not treated on the first instance when the body immune system is fighting against it, the tumor will be more deadly if it finally

destroys the body immune system and become malignant. As the mode number is increased, the complexities of the pattern did not change but for the initial rate of folding required to start the tumor growth which actually increases. The pattern found in the simulation is a good indication of the possible physical representation of cancer after its initiation by denaturation. The knowledge of this pattern will enable radiologists to better study nature cancer from its tumor stage just before metastasis. The dynamic nature of the patterns can equally be used to see the different resistant strains of cancer drugs.

7 Conclusion

From our results and as discussed in the previous section, cancer is a consequence of protein denaturation which comes from loss or breakage of hydrogen bonds as a result of increase body reserve temperature. We saw that this temperature change can come from the increase in body metabolic activities which should be discouraged or external environmental temperature. We also saw folding after denaturation should not be automatic because these will lead to increase tumor growth and malignancy. Frequent and sudden body temperature change will result in more severe malignancy than less frequent and gradual temperature changes. Once diagnosed, treatment of tumor should be considered a priority because the body immune system can eventually fight against the tumor and finally get destroyed making the spread or cancer faster.

Competing Interests

Authors have declared that no competing interests exist.

References

[1] Libonati F, Buehler MJ. Advanced structural materials by bioinspiration. Advanced Engineering Materials. 2017;19(5).
DOI: 10.1002/adem.201600787

[2] Abd-Elhak NA, Ali SE, Zaki NL. Innovative modification of traditional burger. Egypt. J. Agric. Res. 2014;92(3).

[3] Kelly SP, Rosenberg PS, Anderson WF, Andreotti G, Younes N, Cleary SD, Cook MB. Trends in the incidence of fatal prostate cancer in the United States by race. European Urology. 2017;71(2):195-201.
DOI: 10.1016/j.eururo.2016.05.011

[4] Wang Z, Xu D, Ding HF, Kim J, Zhang J, Hai T, Yan C. Loss of ATF3 promotes Akt activation and prostate cancer development in a Pten knockout mouse model. Oncogene. 2015;34(38):4975.
DOI: 10.1038/onc.2015.417

[5] Deng X, He G, Liu J, Luo F, Peng X, Tang S, Keller ET. Recent advances in bone-targeted therapies of metastatic prostate cancer. Cancer Treatment Reviews. 2014;40(6):730-738.
DOI: 10.1016/j.ctrv.2014.04.003

[6] Lee GJ, Roseman AM, Saibil HR, Vierling E. A small heat shock protein stably binds heat-denatured model substrates and can maintain a substrate in a folding-competent state. The EMBO Journal. 1997; 16(3):659-671.

[7] Tanford C. Protein denaturation: Part C. Theoretical models for the mechanism of denaturation. In Advances in protein chemistry. Academic Press. 1970;24:1-95.
DOI: 10.1016/S0065-3233(08)60241-7

[8] Bakthisaran R, Tangirala R, Rao CM. Small heat shock proteins: Role in cellular functions and pathology. Biochimica et Biophysica Acta (BBA)-Proteins and Proteomics. 2015;1854(4):291-319.

[9] Suresh S. Biomechanics and biophysics of cancer cells. Acta Biomaterialia. 2007;3(4):413–438. DOI: doi.org/10.1016/j.actbio.2007.04.002

[10] Haque MA, Adhikari B. Drying and denaturation of proteins in spray drying process. Handbook of Industrial Drying. 2015;971-985.

[11] Wright NT. Quantitative models of thermal damage to cells and tissues. In Heat Transfer and Fluid Flow in Biological Processes. 2015;59-76.

[12] Lomiwes D, Farouk MM, Wiklund E, Young OA. Small heat shock proteins and their role in meat tenderness: A review. Meat Science. 2014;96(1):26-40.

[13] Park CS, Liu C, Hall SK, Payne SJ. A thermoelastic deformation model of tissue contraction during thermal ablation. International Journal of Hyperthermia. 2017;1-8.

[14] Kunarayakul S, Thaiphanit S, Anprung P, Suppavorasatit I. Optimization of coconut protein deamidation using protein-glutaminase and its effect on solubility, emulsification, and foaming properties of the proteins. Food Hydrocolloids; 2017.

[15] Oyesanya MO, Atabong TA. A fractional reaction diffusion model for tumor, Journal of the Nigeria Mathematical Society. 2008;27:159-195.

[16] Atabong TA, Oyesanya MO, Agwung-Fobellah D. Stability and bifurcations in a competitive model for tumour development and containment. Tro. J. of biomed. and allied sce. Res. 2007;1(1):25-36.

[17] Atabong TA, Oyesanya MO. Hopf bifrucations in reaction diffusion model for tumour development. J. of the Nig. Ass. of Math. Phy. 2009;14:523-540.

[18] Wang J. Spatiotemporal Patterns of a homogeneous diffusive predator–prey system with holling type III functional response. Journal of Dynamics and Differential Equations. 2017;*29*(4):1383-1409. DOI: 10.1007/s10884-016-9517-7

[19] Gatenby RA, Gawlinski ET. A reaction-diffusion model of cancer invasion. Cancer Research. 1996; 56(24):5745-5753.

[20] Siegel RL, Miller KD, Jemal A. Cancer statistics. CA: A Cancer Journal for Clinicians. 2018;68(1):7-30.

[21] Tarakanova A, Kaplan DL, Buehler J. structure and nanomechanics across the inverse temperature. Signature Redacted. 2017;209.

[22] Boselli F, Freund JB, Vermot J. Blood flow mechanics in cardiovascular development. Cellular and Molecular Life Sciences. 2015;72(13):2545-2559.

[23] Saxon CE, Jones SL, Nakada RM, Churchill C, Maunder C. Do muscle contractile mechanics alter blood flow and explain the onset of muscle fatigue?; 2014.

[24] Ribeiro F, Cabella BCT, Martinez AS. Richards-like two species population dynamics model. Theory in biosciences. 2014;133(3-4):135-143. DOI: 10.1007/s12064-014-0205-z

[25] Golestanian R. Enhanced diffusion of enzymes that catalyze exothermic reactions. Physical Review Letters. 2015;115(10):108102.
DOI: 10.1103/PhysRevLett.115.108102

[26] Sun L, Gidley MJ, Warren FJ. The mechanism of interactions between tea polyphenols and porcine pancreatic alpha-amylase: Analysis by inhibition kinetics, fluorescence quenching, differential scanning calorimetry and isothermal titration calorimetry. Molecular Nutrition & Food Research; 2017.
DOI: 10.1002/mnfr.201700324

[27] Lee I, Kim H, Ko YJ, Lee W. NMR characterization of the DNA-binding domain of arabidopsis thaliana telomere repeat factor. Bulletin of the Korean Chemical Society. 2016;37(4):485-489.
DOI: 10.1002/bkcs.10708.

[28] Kampinga HH. Thermotolerance in mammalian cells. Protein denaturation and aggregation, and stress proteins. Journal of Cell Science. 1993;104:11-17.

[29] Zhelezny VP, Motovoy IV, Ustyuzhanin EE. Prediction of nanofluids properties: the density and the heat capacity. In Journal of Physics: Conference Series. IOP Publishing. 2017;891(1):012347.
DOI: 10.1088/1742-6596/891/1/012347

[30] Pobelov IV, Lauritzen KP, Yoshida K, Jensen A, Mészáros G, Jacobsen KW, Solomon GC. Dynamic breaking of a single gold bond. Nature Communications. 2017;8:15931.

[31] Kong SC, Gianuzzo A, Novak I, Pedersen SF. Acid-base transport in pancreatic cancer: molecular mechanisms and clinical potential. Biochemistry and Cell Biology. 2014;92(6):449-459.
DOI: 10.1139/bcb-2014-0078

[32] Markus JB, Ackbarow T. Fracture mechanics of protein materials. Materials. 2007;10(9):48-58.

[33] WHO. Global health risks: mortality and burden of disease attributable to selected major risks. WHO, Geneva; 2009.

[34] Zhou XN, et al. Potential impact of climate change on schistosomiasis transmission in China. American Journal of Tropical Medicine and Hygiene. 2008;78:188–194.

[35] Robine JM, et al. Death toll exceeded 70 000 in Europe during the summer of 2003. Les Comptes Rendus/Série Biologies. 2008;331:171–78.

[36] Hales S, et al. Potential effect of population and climate changes on global distribution of dengue fever: an empirical model. The Lancet. 2002;360:830–834.

[37] Arnell NW. Climate change and global water resources: SRES emissions and socio-economic scenarios. Global Environmental Change – Human and Policy Dimensions. 2004;14:31–52.

[38] Climate change. Impacts, adaptation and vulnerability. Geneva, Intergovernmental Panel on Climate Change, 2007 (Contribution of Working Group II to the Fourth Assessment Report of the Intergovernmental Panel on Climate Change); 2007.

[39] Qin Z, Balasubramanian SK, Wolkers WF, Pearce JA, Bischof JC. Correlated parameter fit of Arrhenius model for thermal denaturation of proteins and cells. Annals of Biomedical Engineering. 2014;42(12):2392-2404.
DOI: 10.1007/s10439-014-1100-y

[40] Weir HK, Anderson RN, Coleman King SM, Soman A, Thompson TD, Hong Y, et al. Heart Disease and Cancer Deaths — Trends and Projections in the United States, 1969–2020. Prev Chronic Dis. 2016;13:160211.
DOI: http://dx.doi.org/10.5888/pcd13.160211

[41] Asdourian MS, Skolny MN, Brunelle C, Seward CE, Salama L, Taghian AG. Precautions for breast cancer-related lymphoedema: risk from air travel, ipsilateral arm blood pressure measurements, skin puncture, extreme temperatures, and cellulitis. Lancet Oncol. 2016;17(9):392-405.
DOI: 10.1016/S1470-2045(16)30204-2

Peer-review history:
The peer review history for this paper can be accessed here (Please copy paste the total link in your browser address bar)
http://www.sciencedomain.org/review-history/23638